energy&fuels

pubs.acs.org/EF Article

Mathematic Modeling and Performance Analysis of Vanadium Redox Flow Battery

Feng-Chang Gu, Hung-Cheng Chen,* and Kun-Yi Li

Cite This: *Energy Fuels* 2020, 34, 10142−10147 Read Online

ACCESS | Metrics & More | Article Recommendations

ABSTRACT: With a rapid charge/discharge feature, vanadium redox flow batteries (VRBs) are green, large-scale energy storage devices useful for power smoothing in unstable renewable power generation facilities, such as those involving solar and wind energy. This study developed a VRB model to establish a relationship between electrolyte concentration, equilibrium potential, and state of charge (SOC), to simulate the dynamic responses in charge/discharge cycles of the electrolyte concentration, terminal voltage, and SOC, and to evaluate the internal loss and battery efficiency. The proposed model not only serves as the basis of a dynamic analysis tool for future studies for designing a large-scale VRB but also reveals the time-varying electrolyte status for a long-term VRB operation.

1. INTRODUCTION

With the accelerated depletion of fossil fuels, using alternative and renewable energy resources such as solar energy and wind power has become crucial. However, the inevitable intermittence in the use of such alternatives leads to output power fluctuations, which has a severe effect on electricity networks.[1−3] Thus, developing a method to regulate output power to a specified level is critical. In contrast to Cr−Fe, Cd−Ni, and lead−acid batteries, the advantages of redox flow batteries (VRBs) are their simple structure, high state of charge (SOC), and long service life. The VRB is considered a promising green solution for practical applications.[4−7] The VRB is a type of a rechargeable flow battery in which different oxidation states of vanadium ions are used to store chemical potential energy. The ability of vanadium to exist in four oxidation states is exploited in VRBs. Only one electroactive element is present in VRBs. The main advantages of VRBs are as follows: almost unlimited energy capacity simply using large electrolyte storage tanks; VRBs can be allowed to be completely discharged for long periods; an accidental mixture of the electrolytes of batteries does not cause permanent damage; a single state of charge between the two electrolytes avoids capacity degradation due to a single cell in nonflow batteries; and the electrolyte is aqueous and inherently safe and nonflammable. VRBs can be used at a depth of discharge (DOD) of approximately 90% and more, that is, deeper DODs than solid-state batteries (e.g., lithium-based and sodium-based batteries are typically specified with DOD = 80%). In addition, VRBs exhibit considerably long cycle lives: most producers specify cycle durability higher than 15 000−20 000 charge/discharge cycles. For several reasons, including their relative bulkiness, most vanadium batteries are currently used for grid energy storage, that is, power plants or electrical grids. However, VRB exhibits a poor energy-to-volume ratio and poor round trip efficiency compared with standard storage batteries. Furthermore, the aqueous electrolyte renders the battery heavy and is therefore useful only for stationary applications. Another disadvantage is the relatively high toxicity of vanadium oxides.

To regulate the output power provided by power networks or plants, VRB modeling is essential, when designing a VRB system with complex constituents such as an electrolyte circulation system and electrical components, for redox reactions. Several modeling studies in which reactions at electrodes are based on the concentration distribution of an electrolyte solution along the flow vector direction on the surface of charge/discharge cells have been conducted.[8−14] An equivalent circuit model was proposed in reference[15] based on the time constant of an electric response. However, thus far, no model to accurately determine the behavior of a VRB system during a transient state under various loading conditions has been reported; the dynamical responses of the VRB employed in a power network can be estimated numerically or theoretically. This paper describes an electrochemical mechanism obtained through a VRB model constructed on the basis of a prior study that considered all relevant VRB electrochemical properties, including vanadium concentrations, proton concentrations, equilibrium potential, and SOC. THE model was subsequently used to plot both the output voltage and power profiles during charge/discharge cycles. Moreover, by considering the internal loss in the end, battery performances, namely, dynamic responses and operating efficiency, were assessed. Accordingly, the relationship between chemical reactions and electrical characteristics under normal charge/discharge operations was obtained.

Received: May 13, 2020
Revised: July 10, 2020
Published: July 15, 2020

https://dx.doi.org/10.1021/acs.energyfuels.0c01536
Energy Fuels 2020, 34, 10142−10147

2. ELECTROCHEMISTRY OF THE VRB

Current vanadium redox batteries have the following specifications: specific energy of approximately 10−20 Wh/kg (36−72 kJ/kg) of the electrolyte; energy density of 15−25 Wh/L (54−65 kJ/L); time durability of 20−30 years; cycle durability >15 000−20 000 cycles; and nominal cell voltage of 1.15−1.55 V. The VRB is an electrochemical energy storage device that uses a vanadium solution as active material on the cathode and anode. When completely charged, the open-circuit voltages can reach up to 1.5 V. V^{2+}, V^{3+}, V^{4+}, and V^{5+} are the oxidation states of vanadium. In addition, V^{4+} and V^{5+} form the valence states in vanadium oxides VO^{2+} and VO_2^+, respectively.[15] Figure 1 illustrates a redox process of VRB

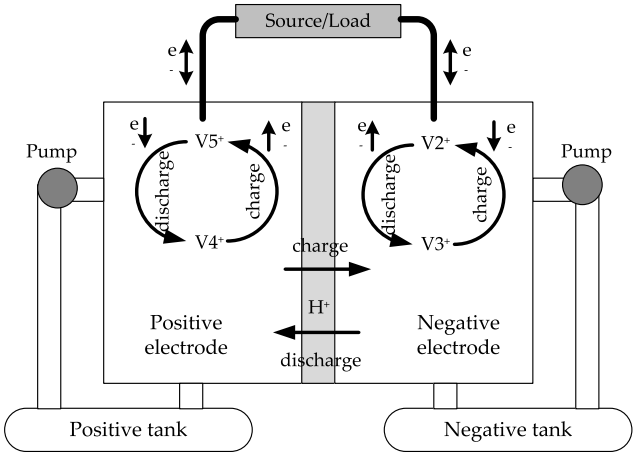

Figure 1. Redox process of the VRB under charge/discharge conditions.

under the charge/discharge condition. Electron (e^-) migrates from the cathode to anode through an external load. Simultaneously, vanadium V^{2+} (catholyte) and V^{5+} (anolyte) change to V^{3+} and V^{4+}, respectively. Protons H^+ flow through an inner membrane in the opposite direction. The migration directions of the same particles during discharging and charging are exactly the opposite.[16,17] The chemical mechanisms are expressed as follows

$$VO_2^+ + 2H^+ + e^- \underset{\text{charge}}{\overset{\text{discharge}}{\rightleftharpoons}} VO^{2+} + H_2O \quad (1)$$

$$V^{2+} \underset{\text{charge}}{\overset{\text{discharge}}{\rightleftharpoons}} V^{3+} + e^- \quad (2)$$

$$VO_2^+ + 2H^+ + e^- \underset{\text{charge}}{\overset{\text{discharge}}{\rightleftharpoons}} VO^{2+} + H_2O + VO^{3+} \quad (3)$$

3. VRB MODEL

Figure 2 illustrates the VRB electrochemical model. The terminal voltage V_b in a VRB is a function of six operating conditions: current I, electrolyte flow rate Q, vanadium concentrations in a cell C_{cv} and a tank C_{tv}, proton concentration C_{H^+}, and temperature T. When the battery current and electrolyte amount are provided, the open-circuit voltage V_{oc}, also known as the equilibrium potential V_{eq}, is

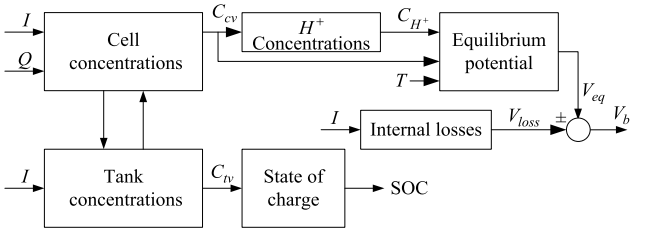

Figure 2. VRB electrochemical model.

determined using the concentrations of hydrogen ions and vanadium present in the electrolyte. Subsequently, the subtraction of the internal loss voltage V_{loss} from V_{oc} yields V_b.[18,19]

3.1. Concentration of Vanadium Ions. The electrolyte flow between the cell and tank causes the concentration to decrease. Consider when the electrolyte mixing time is neglected, the identical mechanism is shared by charge and discharge cycles. The electrolyte flow is constant, and the rate of the concentration change in V^{2+} can be defined as follows:

$$\frac{d[V^{2+}]_C}{dt} = \mp\frac{i}{\alpha_c F} + \frac{Q}{\alpha_C}\{[V^{2+}]_T - [V^{2+}]_C\} \quad (4)$$

where α_C is the electrolyte amount of the VRB, F is the Faraday constant, and i (−/+) is the current during charge/discharge processes. The total amount of vanadium ions V^{2+} can express as

$$\alpha_c[V^{2+}]_C + \alpha_T[V^{2+}]_T = \frac{N}{N_A} \quad (5)$$

where N is the number of V^{2+}, α_T is the amount of the electrolyte in the tank, and N_A is the Avagadro constant. The rate of change in N is related to the current i and can be expressed as follows

$$\frac{1}{N_A}\frac{dN}{dt} = \mp\frac{i}{F} \quad (6)$$

Based on eqs 4−6, the concentration change in V^{2+} can be represented as

$$\frac{d^2[V^{2+}]_C}{dt^2} = -\left\{Q\left(\frac{1}{\alpha_C} + \frac{1}{\alpha_T}\right) - \frac{1}{Q}\frac{dQ}{dt}\right\}\frac{d[V^{2+}]_C}{dt} \mp \frac{i}{\alpha_C F}\frac{di}{dt} \mp \left(\frac{Q}{\alpha_C} - \frac{1}{Q}\frac{dQ}{dt}\right)\frac{i}{\alpha_C F} \quad (7)$$

Assume the flow rate Q is constant at Q_0, then eq 7 can be simplified as

$$\frac{d^2[V^{2+}]_C}{dt^2} = -Q_0\left(\frac{1}{\alpha_C} + \frac{1}{\alpha_T}\right)\frac{d[V^{2+}]_C}{dt} \mp \frac{1}{\alpha_c F}\frac{di}{dt} \mp \frac{Q}{\alpha_C}\frac{i}{\alpha_c F} \quad (8)$$

and the change in the V^{2+} concentration in the tank is expressed as

$$\frac{d[V^{2+}]_T}{dt} = \frac{1}{\alpha_T}\left(-\alpha_C\frac{d[V^{2+}]_C}{dt} \mp \frac{i}{F}\right) \quad (9)$$

https://dx.doi.org/10.1021/acs.energyfuels.0c01536
Energy Fuels 2020, 34, 10142−10147

Figure 3 presents a plot of vanadium concentrations in the cell and tank against the SOC at 25 °C.

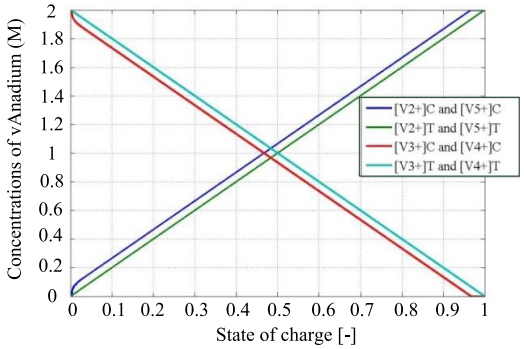

Figure 3. Vanadium concentrations in the cell and tank versus the SOC at 25 °C.

3.2. Concentration of Protons. The electrolyte contains not only vanadium ions but also SO_4^{2} and H^+. Figure 4 illustrates the chemical reaction mechanism and the reason for protons to cross the VRB membrane. Thus, the H^+ concentration influenced by the chemical constituents of anolyte is formulated as

$$[H^+] = [H^+]_{\text{discharged}} + [VO_2^+] \tag{10}$$

where $[H^+]_{\text{discharged}}$ represents the hydrogen ion concentration under the completely discharged condition. Figure 5 presents the plot of proton H^+ concentrations in both the cell and tank against the SOC.

3.3. Equilibrium Potential. Through the Nernst equation, the concentration of electrolyte was found to influence the equilibrium potential of the VRB.[20] When the concentration of vanadium and hydrogen ions in a VRB stack is provided, the equilibrium potential V_{eq} is evaluated as follows

$$E = E' + \frac{RT}{F} \ln \frac{[V^{2+}]_C + [VO_2^+]_C [H^+]_C [H^+]_C}{[V^{3+}]_C [VO^{2+}]_C} \tag{11}$$

where $E \doteqdot 1.255$ V is the standard potential, R the ideal gas constant, and T the temperature. In a completely charged state, the anolyte permits only VO_2^+ but not VO^{2+} ions, and only V^{2+} but not V^{3+} ions are present in the anolyte.

Accordingly, $[VO_2^+]$, the VO_2^+ concentration is equal to $[V^{2+}]$ in the completely charged state, following which $[VO_2^+]$

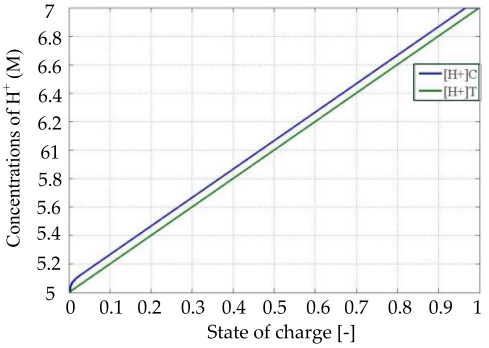

Figure 5. Proton H^+ concentrations in the cell and tank versus the SOC at 25 °C.

$= [V^{2+}]$ and $[VO^{2+}] = [V^{3+}]$ at any given SOC, and eq 11 can be simplified as

$$E = E' + \frac{RT}{F} \ln \frac{[V^{2+}]_C^2 + [H^+]_C^2}{[V^{3+}]_C^2} \tag{12}$$

Figure 6 presents a plot of the equilibrium potential versus the SOC at 25 °C.

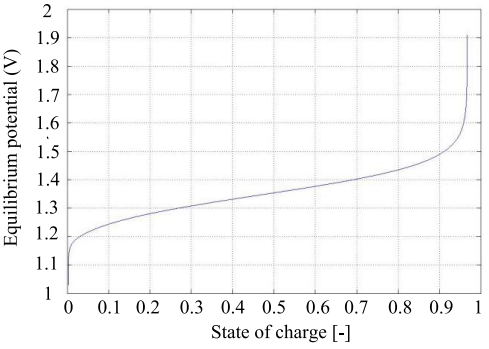

Figure 6. Equilibrium potential versus the SOC at 25 °C.

3.4. Internal Loss Voltage. When the current flows, the difference is generated between the terminal voltage and equilibrium potential. This difference is the internal loss voltage V_{loss}, which is treated as a quantity subjected to the time-varying current I, flow rate Q, and electrolyte temperature T and is presented as

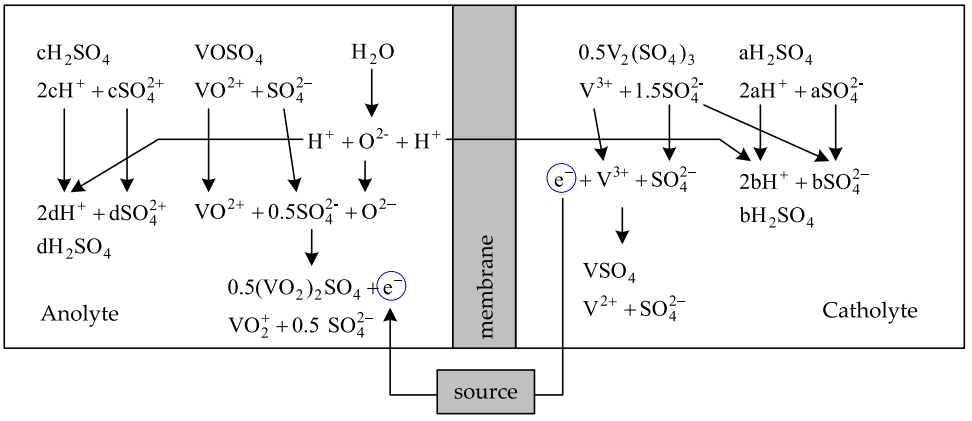

Figure 4. Complete ionic equations of the VRB during charging.

https://dx.doi.org/10.1021/acs.energyfuels.0c01536
Energy Fuels 2020, 34, 10142−10147

$$V_{loss}(I, t, Q, T) = V_{eq} - V_b \quad (13)$$

During simulations, the flow rate Q and temperature T are kept constant. Therefore, eq 13 is simplified as

$$V_{loss}(I, t) = V_{eq} - V_b = R_{discharge/charge} I + \eta_{discharge/charge} \quad (14)$$

where $R_{discharge/charge}$ and $\eta_{discharge/charge}$ symbolize the equivalent series resistance and overpotential during charge/discharge cycles, respectively. Because there is a weak dependence on V_{eq}, $\eta_{discharge/charge}$ is approximated as a constant. Table 1 presents the respective equivalent series resistance and overpotential for each cell stack. Figure 7 presents the equilibrium potential and terminal voltage profiles for a single VRB during complete charge/discharge cycles at 40 A.

Table 1. Equivalent Series Resistance and Overpotential under Charge/Discharge Conditions

state	charge	discharge
R (Ω)	0.00245	0.0028
η (V)	0.0217	0.0067

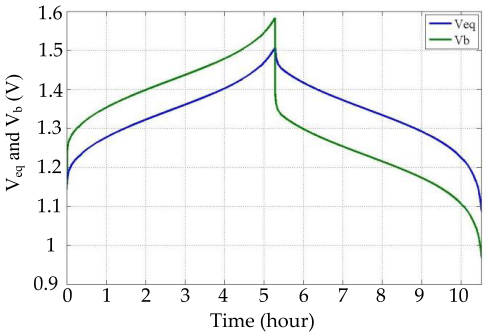

Figure 7. Equilibrium potential and terminal voltage profiles during complete charge/discharge cycles at 40 A.

3.5. State of Charge. SOC, ranging between 0 and 1, refers to a measure of the residual energy in the storage tank (0 = empty and 1 = full). As suggested in reference,[20] SOC is given by

$$SOC = \left(\frac{[VO_2^+]_T}{[VO^{2+}]_T + [VO_2^+]_T}\right) = \left(\frac{[V^{2+}]_T}{[V^{2+}]_T + [V^{3+}]_T}\right) \quad (15)$$

Because $[V^{2+}] = [VO_2^+]$ and $[V^{3+}] = [VO^{2+}]$, an identical level of SOC is found in both the anolyte and catholyte.

3.6. VRB Efficiency. The energy efficiency η_w defined as the ratio of the electricity released during a discharge cycle, W_D (Wh), to the electricity injected into a battery during a charge cycle, W_C (Wh), is employed to evaluate the operation performance of the VRB and is expressed as

$$\eta_w = \frac{W_D}{W_C} = \frac{\int_0^{t_d} i_d(t) v_d(t) dt}{\int_0^{t_c} i_c(t) v_c(t) dt} \quad (16)$$

Considering the power dissipated by a pump for circulating the electrolyte, eq 16 is modified as

$$\eta_w = \frac{W_D - W_{PDL}}{W_C + W_{PCL}} = \frac{\int_0^{t_d} i_d(t) v_d(t) dt - W_{PDL}}{\int_0^{t_c} i_c(t) v_c(t) dt + W_{PCL}} \quad (17)$$

where W_{PDL} and W_{PCL} represent the power required by the pump during discharge and charge cycles, respectively.

4. SIMULATIONS AND DISCUSSION

A battery stack is composed of 19 VRBs with a capacity of 1 L connected in a series. The storage tank, containing both the anolyte and catholyte, and the battery stack provide a volume of 83 L, the total vanadium concentration is 2 mol, and the total flow rate is maintained constant is 3.5 L/m, which is equally divided into 3.5/19 L/m using each battery. With an initial SOC of 2.5%, the battery stack is charged at a constant current until a SOC of 97.5% is reached, and the charged stack is then discharged to the original state, that is, the SOC of 2.5%. Figure 8 presents the plot of the time-varying stack voltages V_{stack} during charge and discharge cycles at diverse currents of 100, 80, 60, 40, 20, and 10 A. V_{stack} increases with the time in the charged state, and subsequently plunges when entering the discharged state because the internal loss voltage V_{loss} in a VRB increases with the current. Figure 9 presents a stack power profile obtained during complete charge/discharge cycles at 40 A, where negative and positive profiles in the first and second halves represent the complete charge/discharge cycle, respectively. The power demonstrated in the charge state is higher than that demonstrated in the discharge state. This difference is attributed to the internal loss and more vitally to the power dissipated by the pump for electrolyte circulation. A

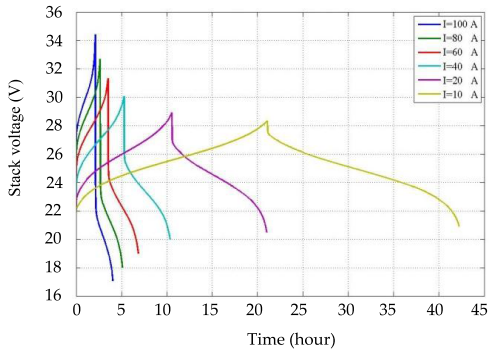

Figure 8. Stack voltages during charge/discharge cycles at diverse currents.

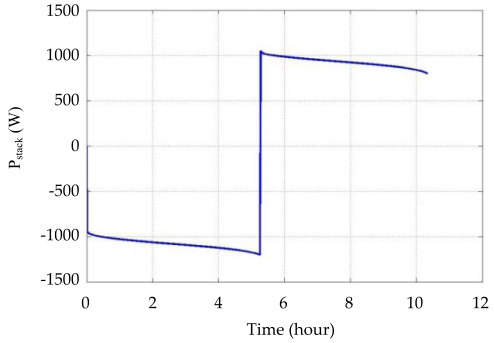

Figure 9. Stack power profile during complete charge/discharge cycles at I = 40 A.

https://dx.doi.org/10.1021/acs.energyfuels.0c01536
Energy Fuels 2020, 34, 10142−10147

fraction of total electricity is delivered to the circulating pump in both charge and discharge states. A flow rate of 3.5 L/m was maintained using the pump, and both W_{PDL} and W_{PCL} were specified at 105 W.

The simulations for the VRB in the discharge state were conducted as follows. Consider an initial electrolyte concentration of 1 mol and an initial SOC of 0.5. The discharge current starts at 30 A; it then increases to 60 A at t = 30 min for a duration of 30 min and subsequently decreases to 20 A. Figures 10−12 present the plots of V^{2+} concentrations in the

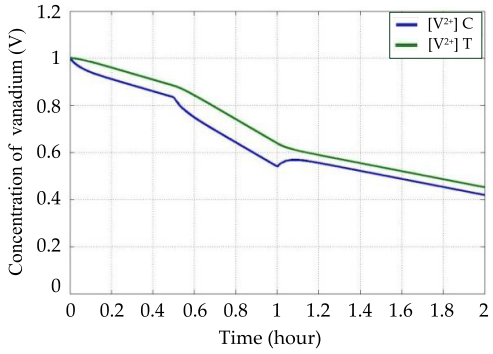

Figure 10. V^{2+} concentration in the discharge state.

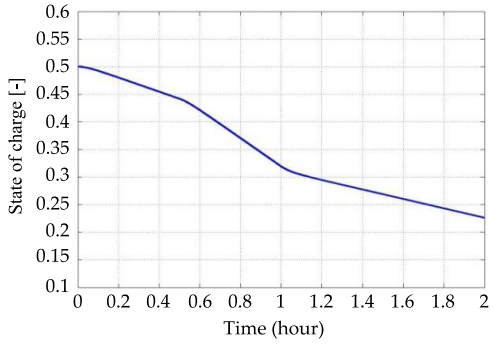

Figure 11. SOC variation in the discharge state.

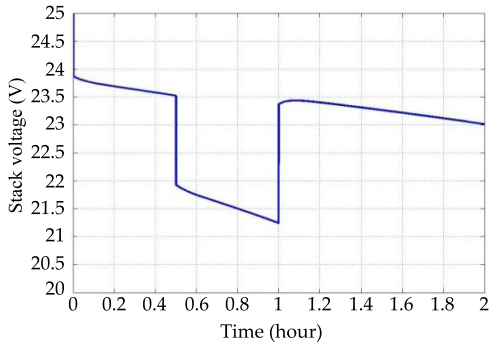

Figure 12. State voltage variation in the discharge state.

cell stack and the tank, SOC, and stack voltage, respectively. Figure 10 indicates that the decrease in concentration between the battery stack and storage tank varies with the discharge current. For instance, at 60 A, the concentration decrease is higher observed than that at 20 A. In addition, the slope of the SOC curve varies with the discharge current (Figure 11). For instance, at 60 A, the drop is steeper than that at 20 A. The abrupt drop at the current transition between 30 and 60 A in the stack voltage accounts for the elevated internal loss voltage (Figure 12). Thus, a rather low stack voltage is maintained until the discharge current decreases to 20 A, and the stack voltage increases subsequently.

The dependence of the energy efficiency on the discharge current in the range of 10−100 A was explored as follows. With the consideration of the internal loss, but not of the pump power consumption of circulating power, Figure 13

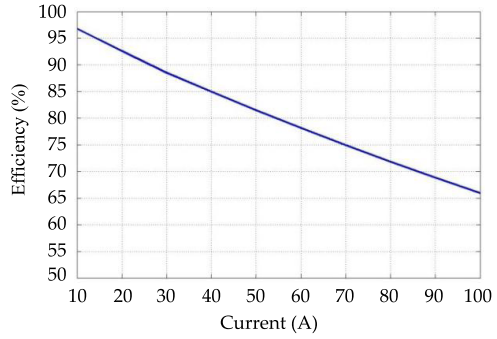

Figure 13. Plot of energy efficiency η_w versus current, with the consideration of pump power dissipation.

indicates that the energy efficiency decreases with the current. The maximum efficiency is observed in the region of 40−50 A, and the minimum efficiency is observed below 10 A, when pump power dissipation is considered (Figure 14), because most of the transferred electricity is drawn using the pump, which reduces the power delivered to the VRB.

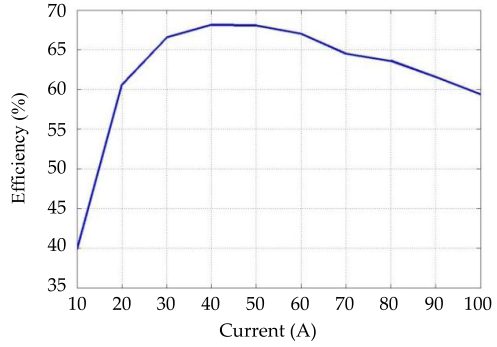

Figure 14. Plot of energy efficiency η_w versus current, with the consideration of pump power dissipation.

5. CONCLUSIONS

A mathematic model based on reaction theory was developed as a base for characterizing the properties of VRBs and analyzing their dynamic responses during charge/discharge cycles. Under various operating conditions, numerous crucial parameters, such as electrolyte concentration, SOC, output voltage, current, and internal loss, can be simulated using this model and applied to simulations of short- and long-term operations when developing a scalable VRB system. A power storage system can be optimized by investigating battery efficiency. For a large-scale VRB, a low ratio between pump power dissipation and total power is observed, which indicates that the efficiency of the entire VRB can be promoted as a green solution for energy storage devices.

https://dx.doi.org/10.1021/acs.energyfuels.0c01536
Energy Fuels 2020, 34, 10142−10147

AUTHOR INFORMATION

Corresponding Author

Hung-Cheng Chen − *Department of Electrical Engineering, National Chin-Yi University of Technology, Taichung 41170, Taiwan, ROC*; Email: hcchen@ncut.edu.tw

Authors

Feng-Chang Gu − *Department of Electrical Engineering, National Chin-Yi University of Technology, Taichung 41170, Taiwan, ROC*; orcid.org/0000-0001-5465-3873

Kun-Yi Li − *Department of Electrical Engineering, National Chin-Yi University of Technology, Taichung 41170, Taiwan, ROC*

Complete contact information is available at: https://pubs.acs.org/10.1021/acs.energyfuels.0c01536

Notes

The authors declare no competing financial interest.

ACKNOWLEDGMENTS

The research was supported by the Ministry of Science and Technology, Taiwan, under Grant Nos. MOST 108-2221-E-167-017 and 108-2622-E-167-005-CC3.

REFERENCES

(1) Liu, B.; Jiang, Y.; Wang, H.; Ge, J.; Shi, H. Sulfonated Poly(ether ether ketone) Hybrid Membranes with Amphoteric Graphene Oxide Nanosheets as Interfacial Reinforcement for Vanadium Redox Flow Battery. *Energy Fuels* **2020**, *34*, 2452−2461.

(2) Hanley, E. S.; Amarandei, G.; Glowacki, B. A. Potential of Redox Flow Batteries and Hydrogen as Integrated Storage for Decentralized Energy Systems. *Energy Fuels* **2016**, *30*, 1477−1486.

(3) D'Agostino, R.; Baumann, L.; Damiano, A.; Boggasch, E. A Vanadium-Redox-Flow-Battery Model for Evaluation of Distributed Storage Implementation in Residential Energy Systems. *IEEE Trans. Energy Convers.* **2015**, *30*, 421−430.

(4) Lei, J.; Gong, Q.; Liu, J.; Qiao, H.; Wang, B. Optimal Allocation of a VRB Energy Storage System for Wind Power Applications Considering the Dynamic Efficiency and Life of VRB in Active Distribution Networks. *IET Renewable Power Gener.* **2019**, *13*, 563−571.

(5) Xiong, B.; Zhao, J.; Su, Y.; Wei, Z.; Skyllas-Kazacos, M. State of Charge Estimation of Vanadium Redox Flow Battery Based on Sliding Mode Observer and Dynamic Model Including Capacity Fading Factor. *IEEE Trans. Sustainable Energy* **2017**, *8*, 1658−1667.

(6) Martínez, M.; Molina, M. G.; Mercado, P. E. Optimal Sizing Method of Vanadium Redox Flow Battery to Provide Load Frequency Control in Power Systems with Intermittent Renewable Generation. *IET Renewable Power Gener.* **2017**, *11*, 1804−1811.

(7) Das, B. K.; Al-Abdeli, Y. M.; Woolridge, M. Effects of Battery Technology and Load Scalability on Stand-alone PV/ICE Hybrid Micro-grid System Performance. *Energy* **2019**, *168*, 57−69.

(8) Gautam, R. K.; Kapoor, M.; Verma, A. Tactical Surface Modification of a 3D Graphite Felt as an Electrode of Vanadium Redox Flow Batteries with Enhanced Electrolyte Utilization and Fast Reaction Kinetics. *Energy Fuels* **2020**, *34*, 5060−5071.

(9) Ontiveros, L. J.; Suvire, G. O.; Mercado, P. E. Power Conditioning System Coupled with a Flow Battery for Wind Energy Applications: Modelling and Control Design. *IET Renewable Power Gener.* **2017**, *11*, 987−995.

(10) Noack, J.; Wietschel, L.; Roznyatovskaya, N.; Pinkwart, K.; Tübke, J. Techno-economic Modeling and Analysis of Redox Flow Battery Systems. *Energies* **2016**, *9*, No. 627.

(11) Xie, Z.; Xiong, F.; Zhou, D. Study of the Ce^{3+}/Ce^{4+} Redox Couple in Mixed-Acid Media (CH_3SO_3H and H_2SO_4) for Redox Flow Battery Application. *Energy Fuels* **2011**, *25*, 2399−2404.

(12) Qiu, X.; Crow, M. L.; Elmore, A. C. A Balance-of-plant Vanadium Redox Battery System Model. *IEEE Trans. Sustainable Energy* **2015**, *6*, 557−564.

(13) Nguyen, T. A.; Qiu, X.; Guggenberger, J. D.; Crow, M. L.; Elmore, A. C. Performance Characterization for Photovoltaic-vanadium Redox Battery Microgrid Systems. *IEEE Trans. Sustainable Energy* **2014**, *5*, 1379−1388.

(14) He, G.; Chen, Q.; Kang, C.; Xia, Q. Optimal Operating Strategy and Revenue Estimates for the Arbitrage of a Vanadium Redox Flow Battery Considering Dynamic Efficiencies and Capacity Loss. *IET Gener. Transm. Distrib.* **2016**, *10*, 1278−1285.

(15) Blanc, C.; Rufer, A. In *Optimization of the Operating Point of a Vanadium Redox Flow Battery*; IEEE Energy Conversion Congress and Exposition: San Jose, California, Sept 20−24, 2009; pp 2600−2605.

(16) Cho, H.; Krieg, H. M.; Kerres, J. A. Performances of Anion-exchange Blend Membranes on Vanadium Redox Flow Batteries. *Membranes* **2019**, *9*, No. 31.

(17) Lei, J.; Gong, Q. Operating Strategy and Optimal Allocation of Large-scale VRB Energy Storage System in Active Distribution Networks for Solar/wind Power Applications. *IET Gener. Transm. Distrib.* **2017**, *11*, 2403−2411.

(18) Blanc, C.; Rufer, A. In *Multiphysics and Energetic Modeling of a Vanadium Redox Flow Battery*; IEEE International Conference on Sustainable Energy Technologies: Singapore, Nov 24−27, 2008; pp 696−701.

(19) Nguyen, T. A.; Crow, M. L.; Elmore, A. C. Optimal Sizing of a Vanadium Redox Battery System for Microgrid Systems. *IEEE Trans. Sustainable Energy* **2015**, *6*, 729−737.

(20) Li, M.; Hikihara, T. A Coupled Dynamical Model of Redox Flow Battery Base on Chemical Reaction, Fluid Flow, and Electrical Circuit. *IEICE Trans. Fundam. Electron., Commun. Comput. Sci.* **2008**, *E91-A*, 1741−1747.